JPhys Materials

OPEN ACCESS

RECEIVED
17 November 2019

REVISED
23 January 2020

ACCEPTED FOR PUBLICATION
29 January 2020

PUBLISHED
17 February 2020

PAPER

Kagome metal-organic frameworks as a platform for strongly correlated electrons

Marius Fuchs[1], **Peitao Liu**[2], **Tilman Schwemmer**[1], **Giorgio Sangiovanni**[1], **Ronny Thomale**[1], **Cesare Franchini**[2,3] **and Domenico Di Sante**[1]

[1] Institut für Theoretische Physik und Astrophysik, Universität Würzburg, Am Hubland Campus Süd, Würzburg, D-97074, Germany
[2] University of Vienna, Faculty of Physics and Center for Computational Materials Science, Sensengasse 8, A-1090 Vienna, Austria
[3] Dipartimento di Fisica e Astronomia, Università di Bologna, 40127 Bologna, Italy

E-mail: ddisante@physik.uni-wuerzburg.de

Keywords: electronic correlations, Kagome lattice, organic materials, *ab initio* calculations, constrained random phase approximation

Abstract

By using first-principles calculations we put forward the Cu-dicyanoanthracene lattice as a platform to investigate strong electronic correlations in the family of Kagome metal-organic frameworks. We show that the low-energy model is composed by molecular orbitals which arrange themselves in a typical Kagome lattice at $n = 2/3$ filling, where the Fermi level lies at the Dirac point. The Coulomb interaction matrix expressed in this molecular orbitals basis, as obtained by large-scale constrained random-phase approximation calculations, is characterized by local U and non-local U' parameters exceeding more than ten times the Kagome bandwidth. For such Kagome systems, our findings suggest the possible emergence of peculiar electron–electron collective phenomena, such as an exotic valence bond solid order characterized by modulated bond strengths.

Introduction

Since the discovery of unconventional collective phenomena in high-T_c cuprates, superconducting pairing mechanisms driven by electron–electron interactions have become a predominant center of contemporary research [1]. Interpreting the Fermi surface as a reference infrared fixed point, it is assumed that the bare Coulomb interaction, while repulsive when looked at from an energy scale beyond the electronic bandwidth, develops attractive pairing channels, and hence a Fermi surface instability, as the high-energy (short-wavelength) modes are integrated out towards the Fermi level [2].

The interplay between correlations and complex fermiology can give rise to several collective phenomena in systems with reduced dimensionality, where nesting effects and enhanced quenching of the electron–electron interaction are more effective than in higher dimensions. In the limit of weak coupling, where asymptotically exact expansions exist, superconductivity naturally emerges as the dominant instability of the Fermi surface [3, 4]. At intermediate and strong coupling regimes, however, often at commensurate filling and most preferably around half filling, other kinds of instabilities, such as the condensation of particle–hole pairs, can become competitive or even favorable to superconductivity. This would result in magnetic or charge orders, manifesting themselves in the appearance of spin or charge density waves. Upon doping or external perturbations such as pressure and strain, superconductivity can eventually show up as an effective descendant from the parent phase [5].

Among the existing two-dimensional lattices, the Kagome lattice plays a somewhat special role, since it features an intimate link between sublattice degrees of freedom and interactions at all coupling strengths. In the strong coupling regime, spin disordered phases arise from quantum spin fluctuations of the resulting Kagome spin model at half-filling [6]. Fractional fillings upon doping are further characterized by valence bond order [7]. Doping to the flat band eventually leads to ferromagnetic instabilities [8]. At weak to intermediate couplings, details of the fermiology conspire with electron–electron interactions to reveal a plethora of unconventional phases. Besides the sublattice interference mechanism which at infinitesimal coupling has been shown to favor

exotic superconducting *f*-wave pairing [9], intermediate coupling calculations have predicted several peculiar particle–hole condensates, including finite angular momentum (spin, charge) density waves, as well as a *d*-wave Pomeranchuk instability [10, 11].

Despite this wealth of competing phases, only a handful of materials are known to host realizations of the microscopic Kagome lattice model. The Herbertsmithites such as $ZnCu_3(OH)_6Cl_2$ are an important class of candidates [12, 13], although no conclusive experimental evidence is available to judge the relevance of charge fluctuations and the behavior of the system upon doping [14]. Synthetic metamaterials, such as optical Kagome lattices made of ultracold atoms, furthermore appear as promising alternative routes [15].

In this work we turn our attention to a different and complementary direction to support unconventional many-body phases on the Kagome lattice. Focusing on two-dimensional metal-organic frameworks (MOFs), we show that experimentally available organometallic hybrids [16–19], where metal atoms bond with neighboring molecular groups, promise themselves to be a playground to investigate novel collective electronic phenomena. At the explicit example of Cu-dicyanoanthracene (hereafter Cu-DCA), we have performed *ab initio* calculations to single out, within the framework of the constrained random-phase approximation, the Coulomb interaction matrix in the basis of the low-energy Kagome molecular orbitals. Remarkably, regardless of the pronounced delocalization of such Wannier functions, we obtain significant values for local and non-local Coulomb repulsion.

Compared to inorganic materials, organic systems such as MOFs potentially allow for an easier fine-tuning of parameters in order to adjust and engineer the desired properties [20]. Indeed, multiferroic behaviors and a strong magnetoelectric coupling have been predicted in MOFs [21–24], and electric and magnetic degrees of freedom are further intertwined with optical excitations [25]. However, not much is known so far on the electronically mediated interactions, the interplay between small bandwidth and interaction range, or screening effects. This is the niche where our work places itself in order to provide a new viewpoint on Kagome lattice instabilities, and valuable guidelines for future theoretical and experimental investigations.

Electronic properties

A monolayer of Cu-DCA consists of dicyanoanthracene molecules made of three carbon rings and two CN groups forming a Kagome lattice, as shown in figure 1. The presence of a lone pair in each CN group facilitates the formation of strong coordination bonds with transition metal atoms. In the specific case of Cu-DCA, copper atoms form a regular honeycomb lattice (dark blue spheres in figure 1). The choice of copper is dictated by the recent experimental reports of monolayer Cu-DCA grown on metallic Cu(111) substrate [26, 27].

To characterize the single-particle electronic properties of Cu-DCA we employed density functional theory (DFT) based calculations within the framework of the PBE generalized-gradient-approximation [28], as implemented in the Vienna *ab initio* simulation package (VASP) [29, 30]. The PAW potentials were used [31], and the plane-wave cutoff for the orbitals was chosen to be 400 eV. The Brillouin zone was sampled with a Γ-centered $5 \times 5 \times 1$ mesh of *k*-points, while spin–orbit coupling (SOC) was neglected, since we are not interested here in the physics arising from relativistic electrons. Altough the expected influence of SOC on the Dirac semimetallic character of the Kagome bands is ∼3 meV, a recent study has put forward Cu-DCA as a prime example of intrinsic two-dimensional organic topological insulator [32]. From a broader perspective, topological properties of Kagome and honeycomb MOFs are nowadays attracting considerable interest [33–36], with the scope of broadening and enlarging the technological impact of topological insulators.

Each Cu atom in the unit cell provides the three DCA molecules with a single electron, such that the resulting Kagome low-energy model is formally at $n = 2/3$ electron filling. This is evident from the band dispersion shown in figure 2, where the Fermi level (E_F) sits precisely at the Dirac point of the Kagome manifold, leading to a linearly vanishing DOS at E_F. The two van-Hove singularities, originating from the saddle dispersions at the M points in the Brillouin zone, are characterized by the two symmetric peaks in the DOS at ∼50 meV from E_F. The almost perfectly flat band occupies the topmost part of the spectrum.

As expected from the simple electron counting in the Cu-DCA system, this low-energy Kagome manifold is primarily constituted by orbital contributions from the DCA molecule. To make such a statement formal, we project the three DFT Kohn–Sham wavefunctions $\psi_{n\mathbf{k}}(\mathbf{r})$ (where $n = 1, 2, 3$ refers to the three Kagome bands shown in figure 2) onto a set of three localized p_z^m orbitals, each one centered on the central benzene ring of the *m*th DCA molecule. The resulting overlap matrix $A^{\mathbf{k}}_{nm} = \langle \psi_{n\mathbf{k}} | p_z^m \rangle$ is then used to construct the initial smooth-gauge rotation matrix $\Lambda^{\mathbf{k}}_{nm}$ which allows to define the three molecular Wannier functions $w_{m\mathbf{R}}(\mathbf{r})$ via the lattice Fourier transform

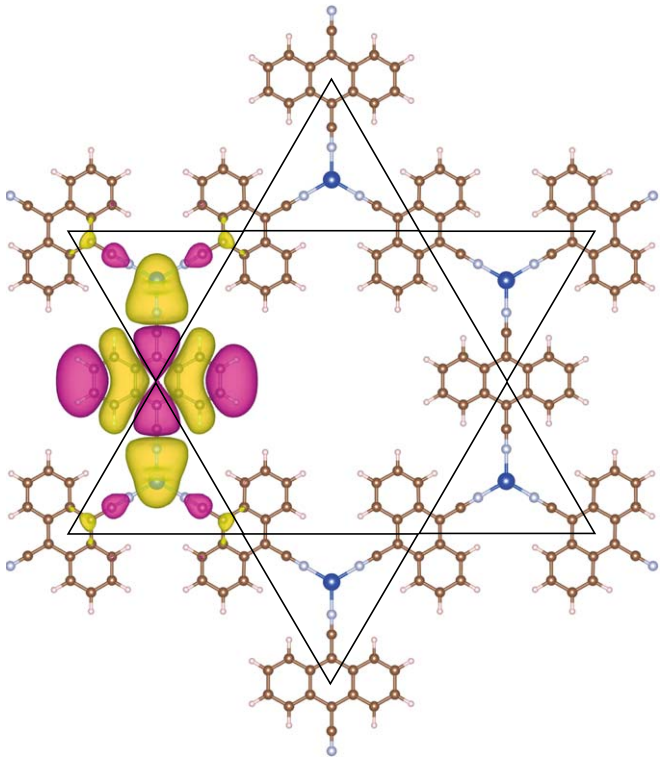

Figure 1. Atomic structure of Kagome Cu-DCA lattice. The DCA molecules form a Kagome texture, and the low-energy electronic dispersion is described by three molecular Wannier functions, each centered around a DCA molecule. One of those is shown, where purple and yellow colors refer to the positive and negative lobes of the Wannier orbital.

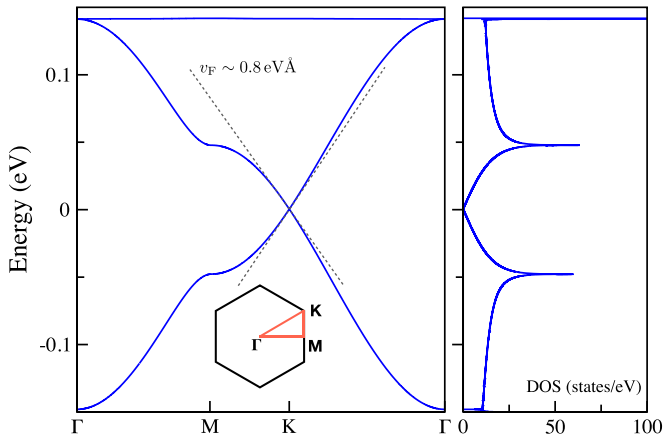

Figure 2. Electronic band structure and density-of-states (DOS) of the low-energy model of Cu-DCA. The zero of the energy scale refers to the Fermi level, which at pristine $n = 2/3$ filling pins to the Dirac point. The inset shows the Brillouin zone of the Kagome lattice and the high-symmetry lines in the irreducible wedge.

$$w_{m\mathbf{R}}(\mathbf{r}) = \frac{\Omega}{(2\pi)^3}\int_{\text{BZ}} d^3\mathbf{k} e^{-i\mathbf{k}\mathbf{R}}\sum_{n=1}^{3}\Lambda^{\mathbf{k}}_{nm}\psi_{n\mathbf{k}}(\mathbf{r}), \tag{1}$$

where Ω is the unit cell volume and $\mathbf{R}$ identifies the Bravais lattice sites. We used the VASP2WANNIER90 interface [37] and the Wannier functions formalism developed and implemented in [38, 39]. In absence of SOC, the Wannier functions are real-valued defined. In figure 1 we show one of the three, which can be easily interpreted as superatomic orbitals contributing to the low-energy description.

This analysis reduces the description of the low-energy electronic properties of Cu-DCA to that of a lattice Kagome model where the effective orbital degrees of freedom are played by the Wannier functions $w_{m\mathbf{R}}(\mathbf{r})$. The resulting non-interacting tight-binding Hamiltonian up to the third nearest neighbor hopping term is given by

$$H^0 = -\sum_{n=1}^{3} t_n \sum_{\langle ij \rangle_n} c_i^\dagger c_j, \tag{2}$$

with $t_1 = 47.76$ meV, $t_2 = 0.36$ meV and $t_3 = 0.34$ meV. Our results are in very good agreement with those reported by Zhang *et al* in [32]. The about two orders of magnitude difference between the nearest neighbor t_1 and longer range neighbor terms suggests that Cu-DCA represents the case of an almost perfect Kagome model. In such a limit, upon inclusion of electronic correlations, nesting effects and sublattice interference are known to drive exotic quantum phases of matter upon doping [9], while a long-sought valence bond solid order is expected as the ground state at pristine filling [7] (see Discussion section).

Constrained random-phase approximation

A primary aim of our study is to set up a Hamiltonian of interacting electrons that faithfully represents the low-energy electronic degrees of freedom of Cu-DCA. In particular, we need to compute the strength of the Coulomb repulsion experienced by charge carriers in the states close to the Fermi level (figure 2). In a solid, the polarizability of charges screens the bare Coulomb repulsion $\mathcal{V}(\mathbf{r}, \mathbf{r}') = \frac{e^2}{4\pi\epsilon_0} 1 \Big/ |\mathbf{r} - \mathbf{r}'|$ and thus the effective screened Coulomb interaction is reduced. When setting up a Hamiltonian for low-energy excitations, its Coulomb interaction needs to be screened by all the excitations that are not included in that Hamiltonian.

A successful approach to disentangle and determine screening effects for the Coulomb interaction is the constrained random phase approximation (cRPA) [40]. To be consistent with the Hamiltonian of equation (2), here we (i) include all contributions to the charge polarization except for those that are confined (constrained) to the subspace of low-energy DCA Kagome bands, and (ii) express the partially screened Coulomb interaction in the basis of molecular Wannier orbitals $w_{m\mathbf{R}}(\mathbf{r})$.

The central idea of cRPA is to remove the contribution χ^c in the target correlated manifold of DCA from the total polarizability χ.

$$\chi^r = \chi - \chi^c. \tag{3}$$

The matrix elements U_{ijkl} of the screened Coulomb interaction expressed in the basis of Wannier functions are given by

$$U_{ijkl} = \lim_{\omega \to 0} \int\int d^3\mathbf{r} d^3\mathbf{r}' w_{i\mathbf{0}}^*(\mathbf{r}) w_{j\mathbf{0}}^*(\mathbf{r}') \mathcal{U}(\mathbf{r}, \mathbf{r}', \omega) w_{k\mathbf{0}}(\mathbf{r}) w_{l\mathbf{0}}(\mathbf{r}'), \tag{4}$$

where $\mathcal{U}$ is the partially screened interaction kernel related to χ^r via the RPA resummation

$$\mathcal{U} = \frac{\mathcal{V}}{1 - \chi^r \mathcal{V}}. \tag{5}$$

In practical *ab initio* calculations of two-dimensional solids, the screened interaction U_{ijkl} highly depends on the amount of vacuum imposed to screen the spurious out-of-plane coupling between the repeated images in a framework of three-dimensional periodic boundary conditions. From a naive viewpoint, a larger vacuum region results in more localized Wannier orbitals, which in turn experience a larger Coulomb repulsion. This trend is corroborated by our simulations in figure 3, where we show the $1/c \to 0$ linear extrapolation of the calculated cRPA values. The extrapolated local interaction $U = U_{1111} = U_{2222} = U_{3333}$ and non-local interaction $U' = U_{1212} = U_{1313} = U_{2323}$ amount to 3.99 eV and 2.52 eV, respectively. These numbers, being one order of magnitude larger than the electronic bandwidth of the Kagome states, put forward Cu-DCA as an ideal platform to study strongly correlated electrons in a two-dimensional MOF, enriching the potentials of the recent field of MOFtronics [41]. Our analysis, however, assumes a freestanding layer of Cu-DCA, neglecting the effects of the supporting Cu(111) substrate. Its metallic nature can indeed provide a further screening channel, as well as doping via charge carrier transfer.

We would like to stress the numerical challenge of such unprecedented large-scale cRPA calculations because of the large memory demand for the calculation of the polarizability. Since the current cRPA implementation of VASP [42] shows a quartic scaling in the system size (number of plane waves) and a quadratic scaling in the number of k-points, it would be prohibitive to perform cRPA calculations on such large system (80 atoms) with large in-plane lattice parameters $a = b = 20.36$ Å and a suitable vacuum length ($c \approx 10$ Å) without a large-memory supercomputer, though the Γ-point only VASP version is used. For instance, for $c = 10$ Å the total amount of memory required by VASP root rank is already as high as 16 GByte. Fortunately, the recently installed new Vienna Scientific cluster 4 (VSC-4) with 768 GByte per fat node (48 cores/node) makes such demanding calculations possible. Although the convergence of the cRPA calculated U value is slow with respect to the vacuum length c, the linear behavior of U over $1/c$ allows us to obtain the converged value (corresponding to infinite vacuum length) upon extrapolation, see figure 3.

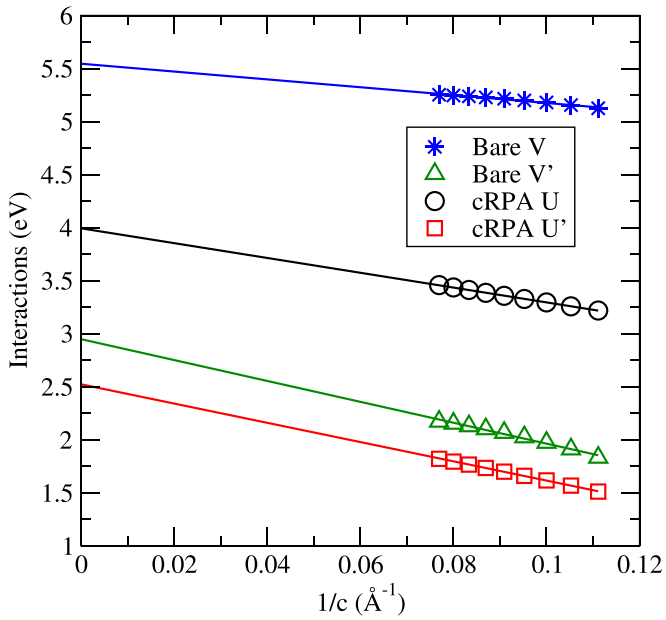

Figure 3. cRPA calculations (circles and squares) and linear extrapolations (solid lines) of the interaction values U and U' as a function of the inverse out-of-plane component of the unit cell $1/c$. The scalings of the bare unscreened on-site interaction V (blue stars) and first-nearest-neighbor interaction V' (green triangles) are likewise shown.

Discussion

Having established the importance of electronic correlations in Cu-DCA, in this section we discuss possible consequences for the ground state properties. A strongly correlated electron system, when the ratio $U/t > 1$, as it is the case for Cu-DCA, can be modeled within the framework of the so-called t-J model. Here electrons hopping on the lattice with probability amplitude t are seen as entities forming localized spin moments interacting via a Heisenberg exchange coupling J. On the Kagome lattice, formed by corner-sharing triangles on a bipartite underlying lattice (triangles are divided in up and down classes, see figure 1), at the Dirac filling of two electrons per triangle ($n = 2/3$), the physical properties have been theoretically proven to be dominated by local states on each triangle [7]. Such states, known as bond-order wave states, belong to the broad category of valence bond solid orders, such as dimerized and plaquette phases, predicted in several frustrated spin models at fractional fillings. The peculiarity of this ground state resides in the fact that it is no longer frustrated, because it minimizes the kinetic and the exchange energy at the same time. Cu-DCA provides a compelling platform to accomplish such an exotic phase of matter, based on the cRPA estimate of the local Coulomb interaction U.

On the other hand, higher order corrections beyond the leading $J = 4t^2/U$ term, as well as non-local Coulomb interaction contributions such as U', could interfere with the dominance of the aforementioned valence bond order, restoring a metallic ground state delocalized from the single triangle local phase of [7]. In particular, charge fluctuations may play an important role and spoil the Heisenberg picture of a spin-only model. In this respect, simple arguments relevant to the case of half-filling suggest a reduction of the effective local interaction to $U_{\text{eff}} = U - U'$ [43], hence lowering the propensity towards the formation of an insulating Mott phase.

To test which consequences a description based on the Hubbard model would have, we have performed cluster dynamical mean field theory (CDMFT) calculations [44–46] in the simplest possible setup. Namely, we have restricted ourselves to three Cu-DCA sites and tiled the two-dimensional Kagome lattice with such minimal cluster. This corresponds to considering CDMFT clusters with just a single unit cell each. Nevertheless it represents one level of complexity above single-site (real-space) DMFT in which the self-energy would be fully site-diagonal. Indeed solving the three-site cluster means that we keep the inter-atomic dependence of the self-energies $\Sigma_{ij}(\omega)$ and describe short-range correlations within the cluster, beyond the local Weiss mean-field theory.

By performing this kind of calculations with and without U' we can infer that the non-local interaction has noticeable consequences on the many-body electronic properties: notwithstanding an increase of the double occupancies $\langle n_{i\uparrow} n_{i\downarrow} \rangle$ on each Kagome site i, we observe a stronger tendency towards the Mott phase upon including U'. This behavior can be understood by noticing that a finite U' increases charge fluctuations, effectively making the system more susceptible to the action of a local interaction U. In an upcoming study we

are going to enlarge the cluster size beyond the minimal three-atom single unit cell geometry considered here. In particular, we would like to see if the reduction of the Mott threshold driven by U' represents a robust result also in the case of larger cluster, for which the effect of the cluster's boundary is weaker than here.

The importance of electronic correlations on the Kagome lattice has been recently emphasized, since strongly correlated Kagome metals have been put forward as convincing platforms to investigate the viscous electron fluid regime [47, 48]. The latter is a current challenge in condensed matter, because it is not amenable to a perturbative description within the framework of the Fermi liquid theory. When the scattering of electrons with impurities and phonons, and related momentum relaxing, is weak, local thermalization from Coulomb interaction becomes the primary mechanism for the formation of an electronic fluid. As a consequence, the dominant time and length scales are controlled by the strength of the Coulomb interaction. At the Dirac filling, this is given by the fine-structure constant

$$\alpha = \frac{e^2}{\epsilon_0 \epsilon_r \hbar v_{\mathrm{F}}}, \tag{6}$$

where ϵ_r and v_{F} are the medium's dielectric constant and the Dirac Fermi velocity, respectively. Estimating from figure 3 and equation (5) that $\epsilon_r = \mathcal{V}/\mathcal{U} \sim 1.38$, and being for Cu-DCA $v_{\mathrm{F}} \sim 0.8$ eV Å, we obtain $\alpha \sim 13$ (for comparison, in graphene $\alpha \sim 1.0$). Interestingly, this large value suggests that organic Kagome metals such as Cu-DCA may also represent suitable platforms to investigate hydrodynamic regimes of the electron fluid, where elusive nonlinear turbulent effects are expected [47].

Conclusion

Using large-scale cRPA simulations, we have investigated the electron–electron interaction properties of Cu-DCA, a recently synthesized Kagome MOF. In spite of the delocalized nature of molecular Wannier orbitals, the Coulomb repulsion is found to be an order of magnitude larger than the low-energy bandwidth. This puts Cu-DCA forward as a potentially relevant Kagome system where collective phenomena driven by electronic correlations could be observed. Moreover, the underlying Kagome lattice offers the opportunity to correlation effects to intertwine with orbital degrees of freedom, eventually leading to exotic ground states of electronic matter. Our analysis, albeit limited to the specific case of Cu-DCA, provides a new viewpoint on organic Kagome lattices and valuable guidelines for future investigations. For example, primed by our findings, a corresponding materials database scan may prove vital to finding related material candidates beyond Cu-DCA.

Acknowledgments

The work is funded by the Deutsche Forschungsgemeinschaft (DFG, German Research Foundation) through Project-ID 258499086—SFB 1170 and through the Würzburg-Dresden Cluster of Excellence on Complexity and Topology in Quantum Matter *ct.qmat* Project-ID 39085490—EXC 2147. The authors gratefully acknowledge the Gauss Centre for Supercomputing e.V. for providing computing time on the GCS Supercomputer SuperMUC at Leibniz Supercomputing Centre (LRZ). Supercomputing time on the Vienna Scientific cluster (VSC) is gratefully acknowledged.

ORCID iDs

Peitao Liu https://orcid.org/0000-0002-6950-1386
Ronny Thomale https://orcid.org/0000-0002-3979-8836
Cesare Franchini https://orcid.org/0000-0002-7990-2984
Domenico Di Sante https://orcid.org/0000-0001-9956-1411

References

[1] Keimer B, Kivelson S A, Norman M R, Uchida S and Zaanen J 2015 *Nature* **518** 179
[2] Shankar R 1994 *Rev. Mod. Phys.* **66** 129
[3] Kohn W and Luttinger J M 1965 *Phys. Rev. Lett.* **15** 524
[4] Raghu S, Kivelson S A and Scalapino D J 2010 *Phys. Rev.* B **81** 224505
[5] Lee P A, Nagaosa N and Wen X-G 2006 *Rev. Mod. Phys.* **78** 17
[6] Misguich G and Lhuillier C 2004 *Frustrated Spin Systems* (Singapore: World Scientific)
[7] Indergand M, Läuchli A, Capponi S and Sigrist M 2006 *Phys. Rev.* B **74** 064429
[8] Tanaka A and Ueda H 2003 *Phys. Rev. Lett.* **90** 067204
[9] Kiesel M L and Thomale R 2012 *Phys. Rev.* B **86** 121105
[10] Kiesel M L, Platt C and Thomale R 2013 *Phys. Rev. Lett.* **110** 126405

[11] Wang W-S, Li Z-Z, Xiang Y-Y and Wang Q-H 2013 *Phys. Rev.* B **87** 115135
[12] Mendels P and Bert F 2010 *J. Phys. Soc. Japan* **79** 011001
[13] Mazin I I, Jeschke H O, Lechermann F, Lee H, Fink M, Thomale R and Valentí R 2014 *Nat. Commun.* **5** 4261
[14] Han T, Chu S and Lee Y S 2012 *Phys. Rev. Lett.* **108** 157202
[15] Jo G-B, Guzman J, Thomas C K, Hosur P, Vishwanath A and Stamper-Kurn D M 2012 *Phys. Rev. Lett.* **108** 045305
[16] Kambe T *et al* 2013 *J. Am. Chem. Soc.* **135** 2462
[17] Sheberla D, Sun L, Blood-Forsythe M A, Er S, Wade C R, Brozek C K, Aspuru-Guzik A and Dincaă M 2014 *J. Am. Chem. Soc.* **136** 8859
[18] Cui J S and Xu Z T 2014 *Chem. Commun.* **50** 3986
[19] Campbell M G, Sheberla D, Liu S F, Swager T M and Dincaă M 2015 *Angew. Chem., Int. Ed.* **54** 4349
[20] Ramesh R 2009 *Nature* **461** 1218
[21] Jain P, Ramachandran V, Clark R J, Zhou H D, Toby B H, Dalal N S, Kroto H W and Cheetham A K 2009 *J. Am. Chem. Soc.* **131** 13625
[22] Di Sante D, Stroppa A, Jain P and Picozzi S 2013 *J. Am. Chem. Soc.* **135** 18126
[23] Stroppa A, Barone P, Jain P, Perez-Mato J M and Picozzi S 2013 *Adv. Mater.* **25** 2284
[24] Stroppa A, Jain P, Barone P, Marsman M, Perez-Mato J M, Cheetham A K, Kroto H W and Picozzi S 2011 *Angew. Chem., Int. Ed.* **50** 5847
[25] Fan F-R, Wu H, Nabok D, Hu S, Ren W, Draxl C and Stroppa A 2017 *J. Am. Chem. Soc.* **139** 12883
[26] Pawin G, Wong K, Kim D, Sun D, Bartels L, Hong S, Rahman T, Carp R and Marsella M 2008 *Angew. Chem., Int. Ed.* **47** 8442
[27] Zhang J, Shchyrba A, Nowakowska S, Meyer E, Jung T A and Muntwiler M 2014 *Chem. Commun.* **50** 12289
[28] Perdew J P, Burke K and Ernzerhof M 1996 *Phys. Rev. Lett.* **77** 3865
[29] Kresse G and Hafner J 1993 *Phys. Rev.* B **47** 558
[30] Kresse G and Furthmüller J 1996 *Phys. Rev.* B **54** 11169
[31] Blöchl P E 1994 *Phys. Rev.* B **50** 17953
[32] Zhang L Z, Wang Z F, Huang B, Cui B, Wang Z, Du S X, Gao H-J and Liu F 2016 *Nano Lett.* **16** 2072
[33] Wang Z F, Liu Z and Liu F 2013 *Nat. Commun.* **4** 1471
[34] Wang Z F, Liu Z and Liu F 2013 *Phys. Rev. Lett.* **110** 196801
[35] Dong L, Kim Y, Er D, Rappe A M and Shenoy V B 2016 *Phys. Rev. Lett.* **116** 096601
[36] Baidya S, Kang S, Kim C H and Yu J 2019 *Sci. Rep.* **9** 13807
[37] Franchini C, Kováčik R, Marsman M, Murthy S S, He J, Ederer C and Kresse G 2012 *J. Phys.: Condens. Matter* **24** 235602
[38] Marzari N, Mostofi A A, Yates J R, Souza I and Vanderbilt D 2012 *Rev. Mod. Phys.* **84** 1419
[39] Mostofi A A, Yates J R, Lee Y-S, Souza I, Vanderbilt D and Marzari N 2008 *Comput. Phys. Commun.* **178** 685
[40] Aryasetiawan F, Imada M, Georges A, Kotliar G, Biermann S and Lichtenstein A I 2004 *Phys. Rev.* B **70** 195104
[41] Dong R *et al* 2018 *Nat. Mater.* **17** 1027
[42] Kaltak M 2015 *PhD Thesis* University of Vienna http://othes.univie.ac.at/38099/
[43] Schüler M, Rösner M, Wehling T O, Lichtenstein A I and Katsnelson M I 2013 *Phys. Rev. Lett.* **111** 036601
[44] Georges A, Kotliar G, Krauth W and Rozenberg M J 1996 *Rev. Mod. Phys.* **68** 13
[45] Maier T, Jarrell M, Pruschke T and Hettler M H 2005 *Rev. Mod. Phys.* **77** 1027
[46] Wallerberger M, Hausoel A, Gunacker P, Kowalski A, Parragh N, Goth F, Held K and Sangiovanni G 2019 *Comput. Phys. Commun.* **235** 388
[47] Di Sante D, Erdmenger J, Greiter M, Matthaiakakis I, Meyer R, Rodríguez Fernández D, Thomale R, van Loon E and Wehling T 2019 arXiv:1911.06810
[48] Polini M and Geim A K 2019 arXiv:1909.10615